

# Tunnelling induced ground settlement considering soil variability

Gouri Krishna <sup>a</sup> and V B Maji <sup>b, \*</sup>

<sup>a</sup> AECOM India, Chennai.

<sup>b</sup> Department of Civil Engineering IIT Madras, Chennai.

Article History:

Received: 15 August 2021.

Revised: 18 July 2022.

Accepted: 12 August 2022.

## ABSTRACT

Ground settlement need to be predicted well so that necessary precautionary measures could be adopted. Ground deformation behavior due to tunnel construction in inhomogeneous soil has been studied in the past few decades by many researchers. When tunnel-induced ground settlement is predicted by considering average soil properties, it is likely to miss the true settlement characteristics and failure mechanism due to the inherent heterogeneity of the ground. In this paper, spatial variability of the ground is considered in the numerical analysis to simulate the ground settlement. A numerical model is developed using the Finite-Difference based numerical code FLAC3D to simulate tunnel construction with earth pressure balance (EPB) TBMs for a case study. Both 2D and 3D random fields are simulated in the numerical model. Results are systematically compared with some of the empirical and analytical methods for predicting ground settlement. Spatial distribution is found to have a significant effect on surface settlements and overall ground behavior.

**Keywords:** Tunnelling, Random field, Spatial variation, Numerical model, FLAC3D.

## 1. Introduction

The ability to predict the tunneling-induced ground settlement in the planning stage is very important to estimate potential damages to infrastructure above and below ground and thereby follow protective measures. There are several relationships available in published literature for the prediction of ground settlement. Ground deformation behavior due to tunnel construction has been broadly studied in past decades by many researchers (Peck, 1969; Attewell and Farmer, 1974; O'Reilly and New, 1982; Sagaseta, 1987; Celestino et al., 2000; Jacobsz et al., 2002; Loganathan and Poulos, 1998). Subsequently, many researchers also advocated the consideration of soil heterogeneity and variability for various geotechnical designs and analyses (Griffiths et al., 2002; Fenton and Griffiths, 2008; Phoon and Kulhawy, 1999 a; Haldar and Mahadevan, 2000). The inherent heterogeneity of ground can be expressed in terms of mean, variance, and scale of fluctuation (SOF) following a probability distribution function, to capture the true failure mechanism due to tunneling. In this paper, numerical models are developed in which spatial variability of soil is modeled through random field modeling. Initially, a two-dimensional (2D) random field is modeled by neglecting the SOF in the third dimension. Since, the tunnel progress in the longitudinal direction, spatial variation in that direction may play a significant role. Though there is a significant development in the field of tunnel settlement and corresponding spatial variability consideration (Zhang, 2022), many of the issues and challenges need to be explored. The 3D numerical analysis was found to be better for stability evaluation and tunnel design, preferably with consideration of the random field (RFs). For better understanding, spatially variable parameters including hydraulic parameters/ seepage must be simulated as RFs for the probabilistic analysis (Zhang, 2022). The correlations among the soil or rock parameters should be carefully considered; if not, the results may deviate significantly from the realistic characteristics of the performances of the tunnel and deep excavations.

Therefore, an attempt is also made to realize the three-dimensional (3D) random field. The significance of heterogeneity in tunnel-induced ground deformation is analyzed through a comparative study between a homogeneous soil model with the model that considered heterogeneity in various formats. The model is developed using the Finite-Difference-based numerical code *FLAC3D* to simulate tunnel construction with an earth pressure balance tunnel boring machine (EPB-TBM) for a case study from Tehran Metro line 7, Iran. The stage-by-stage construction sequence and machine parameters could be successfully simulated in this model.

## 2. Case study location and geology

Tehran Metro Line 7 is almost 27 km in length with 26 stations. It starts from Shahrak-e-Amir-al-momenin in the east of Tehran and is extended parallel to Navvab Safavi Highway toward the north and reaches Saadat Abad district in the north of Tehran (Chakeri and Unver, 2014). The surface settlement for this Line 7 tunnel, South-North Lot, between N7 and O7 stations of the Tehran Metro Line, is investigated in the present study. A building surcharge of 30 kPa exists just above the tunneling. Soil is of 19 kN/m<sup>3</sup> unit weight and further details are tabulated in table 1. The tunnel is of diameter 9.14 m and the axis lies 20.8 m below the surface. Earth pressure balance machines (EPBMs) were used to bore tunnels in this Tehran Metro line. EPBMs control the stability of the tunnel face and subsidence of the ground surface by monitoring and adjusting the pressure inside the excavation chamber (plenum) to achieve a balance with the pressure in front of the cutter head. The pressure in the plenum should be high enough to maintain ground stability and is controlled by a combination of thrust on the cutter head and the rate of removal of material from the plenum via the screw conveyor. The segmental lining is erected after each push and the annular void created due to overcutting is filled with grout (Chapman et al., 2010). Table 2 gives the technical details about the shield machine, lining rings, and grout.

\* Corresponding author: E-mail address: [vbmaji@gmail.com](mailto:vbmaji@gmail.com) (V B Maji).

**Table 1:** Soil properties of Line 7, Tehran metro tunnel, between N7 and O7 stations.

Engineering classification (BSCS*)	Thickness (m)	Cohesion (kPa)	The angle of internal friction ( $\phi$ )	Young's Modulus (MPa)	Poisson's ratio
Fill	1.2	29	35	15	0.3
ML, CL	8	40	27	30	0.35
GML, GCL	11.6	30	35	80	0.27
GWM, GML	Base	20	38	100	0.27

\* British Soil Classification system, (BSCS) - CL Clay, ML silt, GML silt with gravel, GCL clay with gravel, GWM well-graded silty gravel

**Table 2:** Technical parameters of EPBM (Chakeri and Unver, 2014).

Element	Bulk unit weight (kN/m <sup>3</sup> )	Young's modulus (GPa)	Poisson's ratio	Thickness (cm)
Shield machine	78.4	200	0.25	15
Concrete pre-fabricated lining rings	24	22.5	0.15	35
Grout	12	1	0.25	15

### 3. Numerical simulation

#### 3.1. Introduction

The tunnel excavation using the Earth Pressure Balance Tunnel Boring Machine (EPB-TBM) in Tehran Metro line 7 has been numerically simulated using *FLAC3D*, a finite difference-based code (Itasca, 2013) to predict the ground settlement. Considering the symmetry of the tunneling procedure, a half-symmetric model along the longitudinal axis is simulated thereby reducing the computation time. The model has dimensions of 50 x 60 x 50.8 m<sup>3</sup> with a transverse extension of 50m, a longitudinal dimension of 60m, and an extension below the tunnel axis of 30m with a cover depth of 20.8m (Chakeri and Unver, 2014). Displacements were fixed out of the plane direction for all the nodes in boundary planes apart from the plane representing the ground surface ( $z=20.8m$ ) simulating the semi-infinite ground condition. The tunnel is to be excavated in a positive y-direction, starting from  $y = 0m$ . The EPBM properties, as mentioned in Table 2 are used for the analysis. More details on the earlier deterministic numerical analysis with *FLAC3D* can be found in the reference Gouri & Maji (2022). Figure 1 shows the three-dimensional view showing fixities, surcharge, and liner characteristics as used during the earlier deterministic analysis (Gouri & Maji, 2022). Subsequently, soil properties are modeled to follow spatial distribution which is a more realistic simulation of ground geology.

#### 3.2. Random field modeling

Among the soil properties, it is widely accepted that Young's modulus and Poisson's ratio are the dominant ones that greatly affect the deformations of soil. It is also believed that Poisson's ratio has less spatial variability and second-order significance in the prediction of deformation (Fenton and Griffiths, 2008). Other properties are given similar to the stratified soil model (Table 1). A simplification is introduced that only the soil layer surrounding the tunnel, 11.67m above and below the horizontal tunnel axis, is simulated to follow the spatial distribution (Table 3). This assumption is made based on the fact that tunnel deformation is mainly affected by the properties of surrounding soil layers within a distance of 1-2 times the tunnel diameter (Gong et al., 2014). So, Young's modulus is assumed to follow lognormal distribution in the said range, with a mean of 90 MPa (average value of Young's modulus in that depth range) and a coefficient of variance of 10 % (Phoon and Kulhawy, 1999 b). The SOF of soil properties usually differs from each other. The vertical SOF ranges from 0.1 m to 7.14 m, while horizontal SOF range from 3 m to 80 m, indicating the usual horizontally layered nature of soils (Huang et al., 2017). The autocorrelation function or correlation model defines the relation between soil property values at two positions and is a function of lag

distance and SOF. A correlated lognormal random field is to be generated for Young's modulus and further mapped onto the *FLAC3D* model. The steps followed to achieve a random field model are as follows:

(i) A sequence of independent normal random variables with zero mean and unit standard deviation was generated with data points equivalent to the number of zones.

(ii) A correlation matrix following the Gauss Markov model as in Eq.1 was generated which shows the autocorrelation among the property concerning space. Autocorrelation function  $\rho(\tau)$  or correlation model defines the relation between soil property values at two positions and is an exponentially decaying function of lag distance ( $\tau$ ) and SOF ( $\delta$ ).

$$\rho(\tau) = \exp(-2\tau / \delta) \quad (1)$$

(iii) Once the correlation matrix was established, it was decomposed into upper and lower triangular matrices using Cholesky decomposition.

(iv) Correlated standard normal field ( $G_i$ ) was then obtained by multiplying the lower triangular matrix with the sequence of independent normal random numbers, generated in steps (iii) and (i) respectively.

(v) The lognormal mean ( $\lambda$ ) and standard deviation ( $\zeta$ ) are calculated from statistical parameters ( $\mu$  and  $\sigma$ ) of the soil property, based on the lognormal distribution transformation as given by Eq.2 and Eq.3.

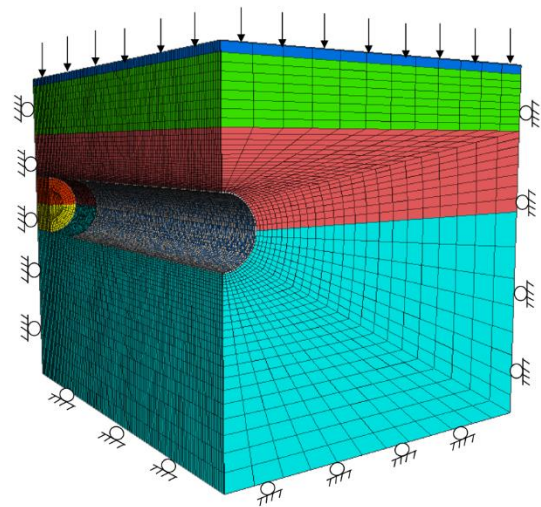


**Figure 1:** Three-dimensional view showing fixities, surcharge and liner (Gouri and Maji, 2022).

**Table 3:** Geotechnical design data for the spatial distribution.

Layer	Engineering classification (BSCS)	Thickness (m)	Unit weight (kg/m <sup>3</sup> )	Cohesion (kPa)	The angle of internal friction (°)	Young's Modulus (MPa)		Poisson's ratio
						Mean	COV (%)	
Layer 1	Fill	1.2	1900	29	35	15	0	0.3
Layer 2	ML, CL	8	1900	40	27	30	0	0.35
Layer 3	GML, GCL	11.67	1900	30	35	90	10	0.27
Layer 4	GWM, GML	11.67	1900	20	38	90	10	0.27
Layer 5	GWM, GML	Base	1900	20	38	100	0	0.27

$$\lambda = \ln(\mu) - (1/2)\zeta^2 \quad (2)$$

$$\zeta^2 = \ln[1 + (\sigma/\mu)^2] \quad (3)$$

(vi) The correlated lognormal distribution with mean and variance can be generated as in Eq.4.

$$x_i = \exp[\lambda + \zeta_i G_i] \quad (4)$$

The generated realization of the lognormal random field is distributed through the zones in an orderly fashion. Identifying the pattern followed by zone IDs in all three directions and capturing the zones for the distribution of property through coding was a strenuous process. The radial zones in the tunnel region and brick zones above and below the tunnel were considered two-dimensional while ignored for three-dimensional spatial distribution as it is outside the scope of the present study. The total computation process and distribution of properties are conducted by developing a program using the *FISH* code in *FLAC3D*.

### 3.3. Two-dimensional random field

The half-symmetric model has been numerically simulated as discussed in the previous section with the same dimensions and 61440 zones. Zonation of the model is done in such a way that radial meshing is adopted in the tunnel region and its periphery. The rest area of the model is filled with brick zones maintaining constant center-to-center distance in the transverse direction.

A two-dimensional random field model I is achieved by ignoring SOF in the third dimension i.e. the spatial distribution achieved in the initial set of zones is repeated in the third dimension. This assumption can be made since tunnel problems are usually treated as plain strain cases. The correlation matrix is generated for the initial set, 30 x 14 zones, which drastically reduces the computation time. The radial zones in the tunnel periphery were clubbed and idealized into brick zones to come up with coding to achieve the distribution. The decrease in the number of zones reduces the array size of all the matrices generated thereby reducing the computation time exponentially.

The SOF of soil properties usually differs from each other. The vertical SOF for Young's modulus ranges from 0.1 m to 7.14 m, while horizontal SOF ranges from 3 m to 80 m, indicating the usual horizontally layered nature of soils (Huang et al., 2017). As SOF of soils varies over a wide range both horizontally and vertically, four cases with different magnitudes of horizontal and vertical SOFs were modeled and are shown in Figure 2. Random fields generated can be termed isotropic when horizontal and vertical SOFs were kept the same and anisotropic when they are different. Because horizontal SOF is often much larger than vertical SOF from site investigations, the anisotropic ratio was kept less than one when random fields were analyzed. The soil domain tends to be horizontally stratified as horizontal SOF becomes increasingly larger than vertical SOF and it tends to look like random distribution with no autocorrelation when both SOFs are smaller and equal.

### 3.4. Three-dimensional (3D) random field

The half-symmetric model has been numerically simulated as discussed in the previous section with the same dimensions with a total

of 12480 zones. Here, SOF in the third dimension is considered and a three-dimensional (3D) random field was obtained. The number of zones is kept less than that of the two-dimensional model to reduce the time taken for the computation of the correlation matrix. Zonation was done similarly to the two-dimensional random field model with a different transverse dimension of 1.5 m for brick zones. The three-dimensional random field generated for  $l_h = 10$  m and  $l_v = 2$  m for Young's modulus with mean = 90 MPa and COV = 10%, denoted as case ANI is shown in figure 3.

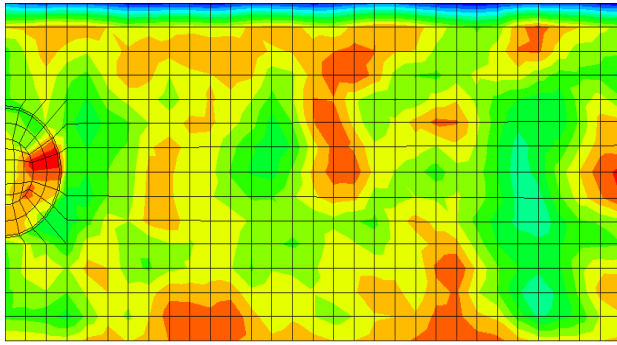
Figure 4 shows the 3D random field generated for case ANI ( $z = 0$  plane). This numerical model was chosen for further analysis and the results are discussed here.

## 4. RESULTS AND DISCUSSION

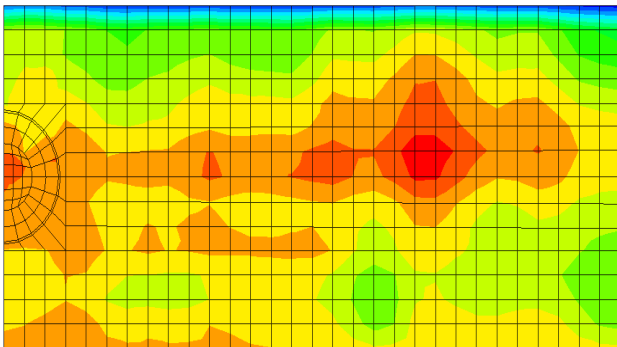
The effect of heterogeneity in ground deformation during the tunneling process is studied through comparison among models following homogeneous, horizontally layered, and spatial distributions. The homogeneous soil model has its soil properties constant value throughout all the zones in the model i.e. an average of all properties in the selected case study. In the horizontally layered soil model, soil properties follow stratified distribution or idealized distribution as given in table 1 while spatial distribution was realized as discussed in section 3, table 3. For ease of discussion, each of the models is going to be denoted with identification names as listed in table 4.

### 4.1. Transverse vertical settlement profile

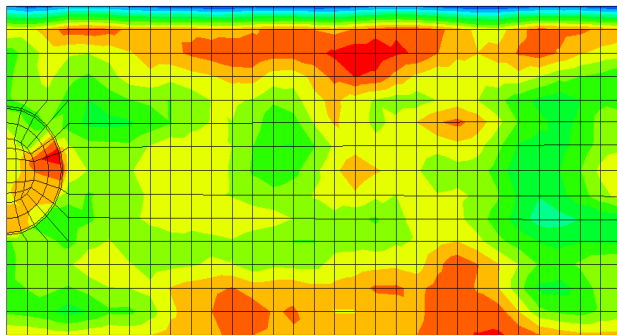
Comparative plots of transverse vertical settlement profiles for models with 2D and 3D random fields along with all other predictions are shown in figures 5 and 6 respectively. Numerical analysis of 2D random field models showed that the shape of the transverse settlement trough obtained for the case of spatially distributed (ANI) is the most conforming to field observations than other cases. The observed settlement data is extrapolated from the maximum vertical settlement value using the Gaussian error function. Empirical and analytical predictions are also plotted along with all the cases for comparison purposes. Peck (1969) is over-predicting while Gonzales and Sagaseta (2001) under-predicted the settlement. The maximum surface settlement of 9.03 mm predicted by case ANI is closer to the observed settlement when compared to the 10 mm predicted by the case of the horizontally layered (LAY) case. Analysis with a homogenous (HOM) layer overestimated the maximum settlement to a value of 11.5 mm. This shows that heterogeneity has a significant influence on the prediction of transverse vertical settlement profiles. Numerical analysis of 3D random field models underestimated the settlement, which could be due to using relatively fewer zones and poor aspect ratios. Analysis in a numerical model with a higher number of zones requires more computation time and due to time constraints, a relatively coarser mesh is adopted. The results of this analysis showed that case HOM is under-predicting the most while cases ANI and LAY are showing almost similar behavior undermining the effect of spatial distribution. More comments can be made on settlement profiles only after an extensive study on models with finer meshing and multiple simulations of random fields with the adoption of Monte Carlo simulations (MCS).



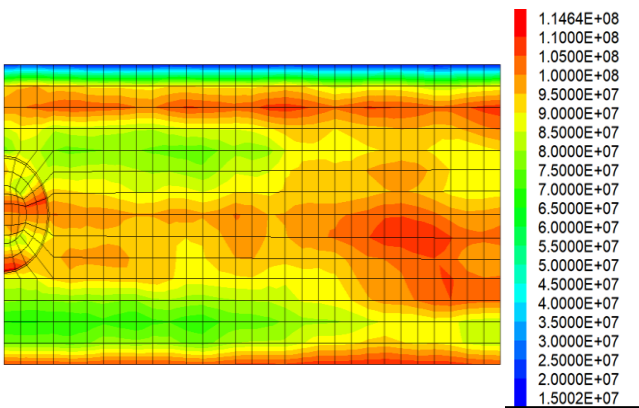
(a)  $l_h = 2$  m and  $l_v = 2$  m



(b)  $l_h = 40$  m and  $l_v = 20$  m



(c)  $l_h = 20$  m and  $l_v = 2$  m



(d)  $l_h = 100$  m and  $l_v = 2$  m

**Figure 2.** Generated random fields (50 m x 23.34 m) of Young's Modulus (Pa) for different SOFs.

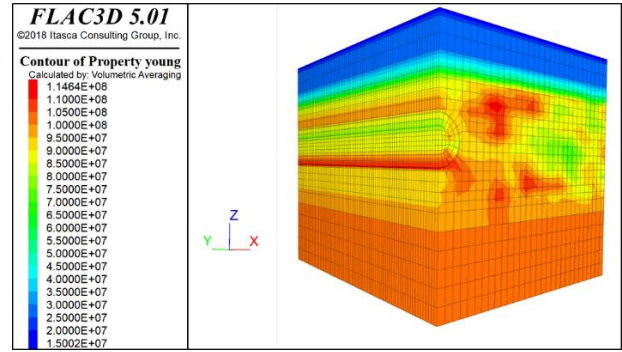


**Figure 3.** Three-dimensional view of generated random field (ANI).

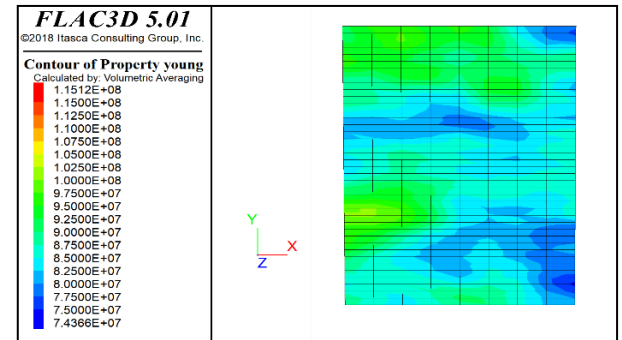


**Figure 4.** Three-dimensional random field generated for case ANI ( $z = 0$  plane).

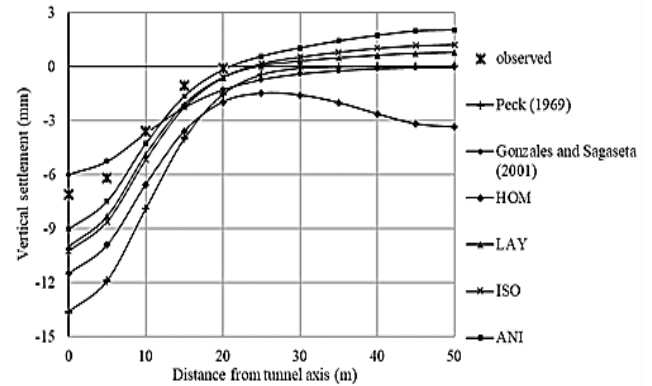


**Figure 5.** Transverse vertical settlement profiles for 2D random field models.

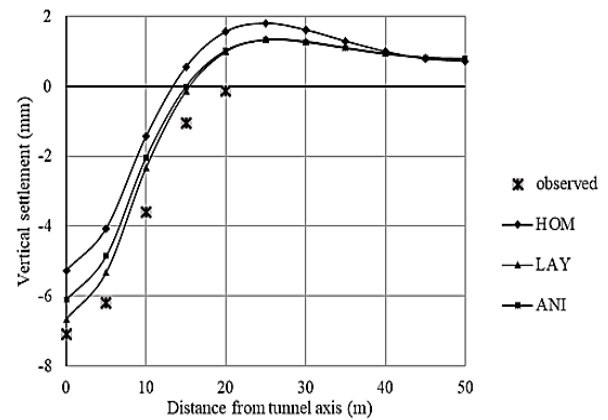


**Figure 6.** Transverse vertical settlement profiles for 3D random field models.

**Table 4:** Numerical models generated for comparative study

Case	Distribution of property
HOM	Homogeneous
LAY	Horizontally layered
ISO	Spatial distribution (lh = 2m, lv = 2m)
ANI	Spatial distribution (lh = 10 m, lv = 2m)

**4.2. Horizontal displacement in the transverse plane**

A numerical analysis of 2D random field models was conducted, and profiles of horizontal displacement (towards the tunnel center line) in the transverse plane are plotted in figure 7. Case HOM is giving the least magnitude of displacement indicating possible underestimation and the profile doesn't match that predicted by O'Reilly and New (1982). The case ISO predicted the highest magnitude of displacement indicating chances of overestimation if SOF values are not chosen properly. Numerical analysis results of 3D random field models compared with profiles of horizontal displacement (towards the tunnel center line) in the transverse plane as shown in figure 8. The profile of horizontal displacement of soil models was similar to that of 2D random field models but lower magnitudes of displacement were predicted later. The reason for this could be attributed to coarser meshing in the models of this study as discussed previously.

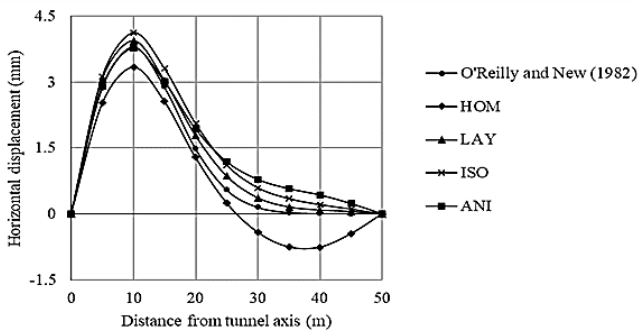


**Figure 7.** Horizontal displacement profiles in the transverse plane (2D random field).

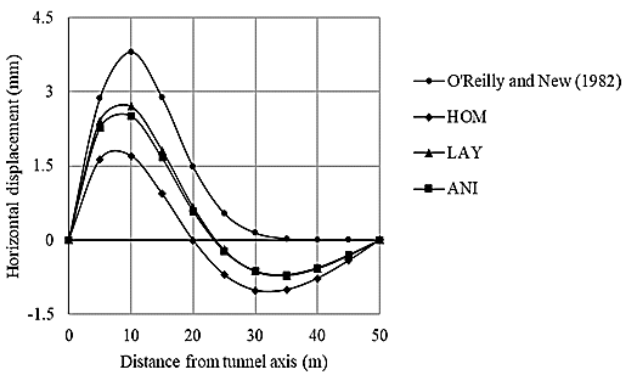


**Figure 8.** Horizontal displacement profiles in the transverse plane (3D random field).

**4.3. Subsurface vertical and horizontal displacement in the transverse plane**

The subsurface vertical and horizontal displacement profiles are shown in figures 9 to 12 for both 2D and 3D random field models. It can

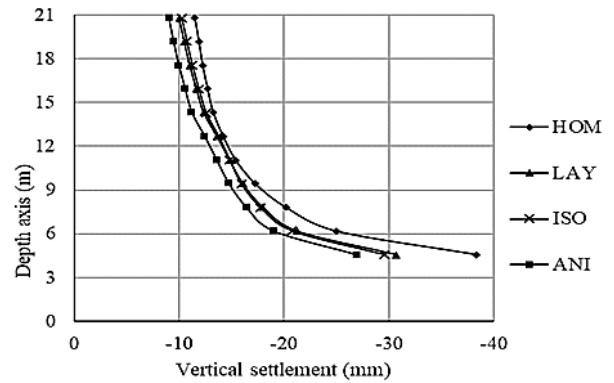


**Figure 9.** Subsurface ver. settlement profile (2D random field).

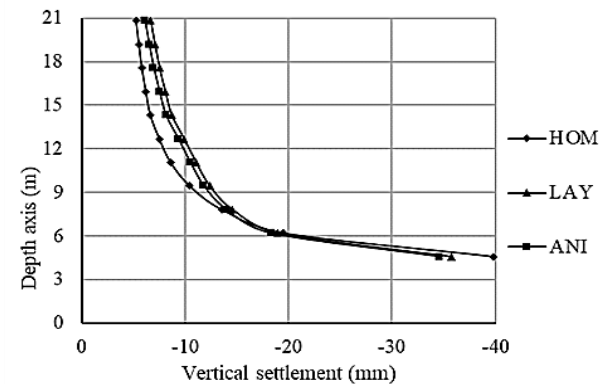


**Figure 10.** Subsurface ver. settlement profile (3D random field).

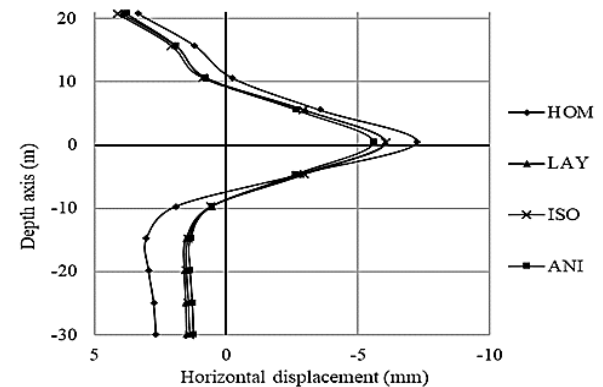


**Figure 11.** Subsurface horizontal displacement profile (2D random field models).

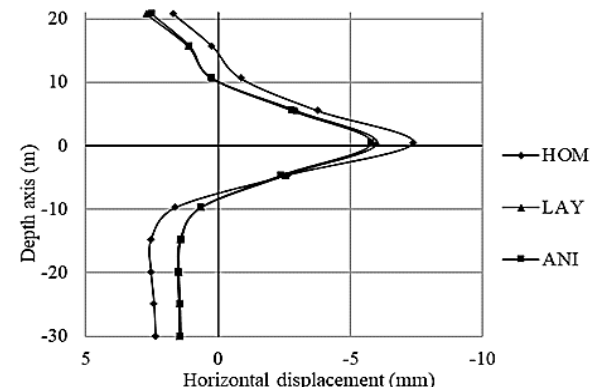


**Figure 12.** Subsurface horizontal displacement profile (3D random field models).

be observed from the figures that a higher magnitude of error exists when average properties are considered for ground deformation prediction as in the case of HOM. Not much difference in magnitude is observed between cases LAY, ISO, and ANI while predicting subsurface displacements. Incorporating spatial variation of property is having an insignificant effect on subsurface deformations concerning this case study and SOF used. The displacement behavior of the model is also subject to the type of meshing adopted and the reliability of statistical parameters used.

## 5. Summery and conclusions

Spatial variability of the ground is considered in the numerical analysis to simulate the ground settlement. In this paper, the effect of heterogeneity in ground deformation during the tunneling process is studied through comparison among models following homogeneous, horizontally layered, and spatial distribution of property. Numerical models were developed to incorporate heterogeneity and spatial variation using *FLAC3D*. The spatial variability of soil was modeled through random field modeling. Initially, two-dimensional (*2D*) random fields were modeled by neglecting the scale of fluctuations (SOF) in the third dimension. Subsequently, attempts were made to realize the three-dimensional (*3D*) random field. *3D* random field modeling is accepted to be more realistic, whereas the results of *2D* random field models are limited by plane strain conditions. Comparative profiles were generated to study the ground behavior under different conditions and it was found that homogeneous distribution causes a considerable deviation. The incorporation of spatial distribution was proved to be ideal while estimating transverse vertical settlement, whereas it is found to have only negligible effect in lateral and subsurface displacements in the present case. The displacement behavior of various models is subject to the type of meshing adopted and the reliability of statistical parameters used. For better prediction, analysis of multiple simulations of the random field is expected. A sensitivity analysis of vertical and horizontal SOF on tunnel deformations is to be conducted to have a better understanding of how spatial variation can affect tunnel-induced ground deformation.

## REFERENCES

- [1] Attewell, P. B., and Farmer, I. W. (1974). "Ground deformations resulting from shield tunnelling in London Clay." *Canadian Geotechnical Journal*, 11(3), pp 380-395.
- [2] Celestino, T. B., Gomes, R. A. M. P., and Bortolucci, A. A. (2000). "Errors in-ground distortions due to settlement trough adjustment." *Tunnelling and underground space technology*, 15(1), pp 97-100.
- [3] Chakeri, H., and Unver, B. (2014). "A new equation for estimating the maximum surface settlement above tunnels excavated in soft ground." *Environmental earth sciences*, 71(7), pp 3195-3210.
- [4] Chapman, D. N., Metje, N., and Stark, A. (2017). *Introduction to tunnel construction*. CRC Press.
- [5] Fenton, G. A., and Griffiths, D. V. (2008). *Risk assessment in geotechnical engineering*, John Wiley and Sons.
- [6] Gong, W., Luo, Z., Juang, C. H., Huang, H., Zhang, J., and Wang, L. (2014). "Optimization of site exploration program for improved prediction of tunneling-induced ground settlement in clays." *Computers and Geotechnics*, 56, pp 69-79.
- [7] González, C., and Sagaseta, C. (2001). "Patterns of soil deformations around tunnels. Application to the extension of Madrid Metro" *Computers and Geotechnics*, 28, pp 445-468.
- [8] Gouri Krishna and Maji, V. B (2022) "Numerical Simulation of EPBM Induced Ground Settlement" *Indian Geotechnical Journal*, 52, pp 341-351.
- [9] Griffiths, D. V., Huang, J., and Fenton, G. A. (2009). "Influence of spatial variability on slope reliability using 2-D random fields." *Journal of geotechnical and geoenvironmental engineering*, 135(10), pp 1367-1378.
- [10] Haldar, A., and Mahadevan, S. (2000). *Probability, reliability, and statistical methods in engineering design*. John Wiley.
- [11] Huang, H. W., Xiao, L., Zhang, D. M., and Zhang, J. (2017). "Influence of spatial variability of soil Young's modulus on tunnel convergence in soft soils." *Engineering Geology*, 228, pp 357-370.
- [12] Itasca Consulting Group, Inc. (2013) *FLAC3D manual (Fast Lagrangian Analysis of Continua in Three dimensions) Version 5.01.154*.
- [13] Jacobsz, S. W., Standing, J. R., Mair, R. J., Hagiwara, T., and Sugiyama, T. (2004). "Centrifuge modeling of tunneling near driven piles." *Soils and Foundations*, 44(1), 49-56.
- [14] Krishna, G., & Maji, V. B. (2022). Numerical Simulation of EPBM Induced Ground Settlement. *Indian Geotechnical Journal*, 52(2), 341-351.
- [15] Loganathan, N., and Poulos, H. G. (1998). "Analytical prediction for tunneling-induced ground movements in clays." *Journal of Geotechnical and geoenvironmental engineering*, 124(9), pp 846-856.
- [16] O'Reilly, M. P., and New, B. M. (1982). "Settlements above tunnels in the United Kingdom-their magnitude and prediction." *The Institution of Mining and Metallurgy, London*, 82, pp 55- 64.
- [17] Peck, R.B. (1969) "Deep excavations and tunneling in soft ground." In *Proceedings 7th International Conference on Soil Mechanics and Foundation Engineering*, State of the Art Volume, pp 225-290.
- [18] Phoon, K. K., and Kulhawy, F. H. (1999 a). "Evaluation of geotechnical property variability." *Canadian Geotechnical Journal*, 36(4), pp 625-639.
- [19] Phoon, K. K., and Kulhawy, F. H. (1999 b). "Characterization of geotechnical variability." *Canadian geotechnical journal*, 36(4), pp 612-624.
- [20] Sagaseta, C. (1987). "Analysis of undrained soil deformation due to ground loss." *Geotechnique*, 37(3), pp 301-320.
- [21] Zhang, W., Han, L., Guc, X., Wang, L., Chen, F. and Liu, H. (2022) "Tunnelling and deep excavations in spatially variable soil and rock masses: A short review" *Underground Space*, 7: 380-407.